NeuroImage: Clinical 27 (2020) 102289

Contents lists available at ScienceDirect

NeuroImage: Clinical

journal homepage: www.elsevier.com/locate/ynicl

Fixel-based analysis links white matter characteristics, serostatus and clinical features in limbic encephalitis

Tobias Bauer[a,1], Leon Ernst[a,1], Bastian David[a], Albert J. Becker[b], Jan Wagner[c], Juri-Alexander Witt[a], Christoph Helmstaedter[a], Bernd Weber[d], Elke Hattingen[e], Christian E. Elger[a], Rainer Surges[a], Theodor Rüber[a,f,g,*]

[a] Department of Epileptology, University Hospital Bonn, Venusberg-Campus 1, 53127 Bonn, Germany
[b] Department of Neuropathology, University Hospital Bonn, Venusberg-Campus 1, 53127 Bonn, Germany
[c] Department of Neurology, University of Ulm and Universitäts- and Rehabilitationskliniken, 89070 Ulm, Germany
[d] Institute of Experimental Epileptology and Cognition Research, University Hospital Bonn, Venusberg-Campus 1, 53127 Bonn, Germany
[e] Department of Neuroradiology, Goethe University Frankfurt, Schleusenweg 2, 60528 Frankfurt, Germany
[f] Epilepsy Center Frankfurt Rhine-Main, Department of Neurology, Goethe University Frankfurt, Schleusenweg 2, 60528 Frankfurt, Germany
[g] Center for Personalized Translational Epilepsy Research (CePTER), Goethe University Frankfurt, Schleusenweg 2, 60528 Frankfurt, Germany

A B S T R A C T

Limbic encephalitis (LE) is an autoimmune syndrome often associated with temporal lobe epilepsy. Recent research suggests that particular structural changes in LE depend on the type of the associated antibody and occur in both mesiotemporal gray matter and white matter regions. However, it remains questionable to what degree conventional diffusion tensor imaging (DTI)-methods reflect alterations in white matter microstructure, since these methods do not account for crossing fibers. To address this methodological shortcoming, we applied fixel-based analysis as a novel technique modeling distinct fiber populations. For our study, 19 patients with LE associated with autoantibodies against glutamic acid decarboxylase 65 (GAD-LE, mean age = 35.9 years, 11 females), 4 patients with LE associated with autoantibodies against leucine-rich glioma-inactivated 1 (LGI1-LE, mean age = 63.3 years, 2 females), 5 patients with LE associated with contactin-associated protein-like 2 (CASPR2, mean age = 57.4, 0 females), 20 age- and gender-matched control patients with hippocampal sclerosis (19 GAD-LE control patients: mean age = 35.1 years, 11 females; 4 LGI1-LE control patients: mean age = 52.6 years, 2 females; 5 CASPR2-LE control patients: mean age = 42.7 years, 0 females; 10 patients are included in more than one group) and 33 age- and gender-matched healthy control subjects (19 GAD-LE healthy controls: mean age = 34.6 years, 11 females; 8 LGI1-LE healthy controls: mean age = 57.0 years, 4 females, 10 CASPR2-LE healthy controls: mean age = 57.2 years, 0 females; 4 subjects are included in more than one group) underwent structural imaging and DTI at 3 T and neuropsychological testing. Patient images were oriented according to lateralization in EEG resulting in an *affected* and *unaffected* hemisphere. Fixel-based metrics fiber density (FD), fiber cross-section (FC), and fiber density and cross-section (FDC = FD · FC) were calculated to retrieve information about white matter integrity both on the micro- and the macroscale. As compared to healthy controls, patients with GAD-LE showed significantly (family-wise error-corrected, $p < 0.05$) lower FDC in the superior longitudinal fascicle bilaterally and in the isthmus of the corpus callosum. In CASPR2-LE, lower FDC in the superior longitudinal fascicle was only present in the *affected* hemisphere. In LGI1-LE, we did not find any white matter alteration of the superior longitudinal fascicle. In an explorative tract-based correlation analysis within the GAD-LE group, only a correlation between the left/right ratio of FC values of the superior longitudinal fascicle and verbal memory performance ($R = 0.64$, Holm-Bonferroni corrected $p < 0.048$) remained significant after correcting for multiple comparisons. Our results underscore the concept of LE as a disease comprising a broad and heterogeneous group of entities and contribute novel aspects to the pathomechanistic understanding of this disease that may strengthen the role of MRI in the diagnosis of LE.

1. Introduction

Limbic encephalitis (LE) is an autoimmune disease characterized by subacute short-term memory loss and psychiatric conspicuity. It often involves temporal lobe epilepsy (Bien and Elger, 2007; Graus et al., 2010; Dalmau and Graus, 2018). To date, a variety of autoantibodies related to different LE subtypes have been identified. Antibodies against the intracellular antigen glutamic acid decarboxylase 65 (GAD) and against the extracellular antigen voltage-gated potassium channel complex (VGKC) rank among the most common autoantibodies associated with LE (Dubey et al., 2018). Within the VGKC-complex, two components that are targeted by different autoantibodies have been found (Irani et al., 2010; Lai et al., 2010; van Sonderen et al., 2017; Binks et al., 2017): Leucine-rich glioma-inactivated 1 (LGI1) and contactin-associated protein-like 2 (CASPR2). Even though different LE subtypes share clinical features, they differ in relevant aspects such as

* Corresponding author.
E-mail address: theodor.rueber@ukbonn.de (T. Rüber).
[1] Equal contribution.

https://doi.org/10.1016/j.nicl.2020.102289
Received 4 December 2019; Received in revised form 22 April 2020; Accepted 24 April 2020
Available online 26 May 2020

Table 1
Demographic- and clinical data of all patient- and control groups. All values are arithmetic group means (range). Verbal memory test: VLMT Helmstaedter et al. (2001), figural memory test: DCS-R Helmstaedter et al. (1991), memory parameters were standardized according to a conormalization sample of 488 healthy volunteers (mean = 100, standard deviation = 10), applying a correction for age. [a]one subject is included in both groups, [b]3 subjects are included in both groups, [c]4 subjects are included in both groups, [d]4 subjects are included in both groups, [e]2 subjects are included in both groups, NA: not applicable, y: years.

	LE			controls			HS			ANOVA
Group	GAD	LGI1	CASPR2	(GAD)	(LGI1)	(CASPR2)	(GAD)	(LGI1)	(CASPR2)	*p*
Number	19	4	5	19[a]	8[b]	10[a,b]	19[c,d]	4[c,e]	5[d,e]	NA
Female (%)	11 (58)	2 (50)	0 (0)	11 (58)	4 (50)	0 (0)	11 (58)	2 (50)	0 (0)	NA
Lateralization right (%)	5 (26)	2 (50)	1 (20)	NA	NA	NA	7 (37)	2 (50)	1 (20)	NA
Age (y)	35.9 (20–61)	63.3 (57–69)	57.4 (40–72)	34.6 (20–50)	57.0 (23–67)	57.2 (44–67)	35.1 (18–59)	52.6 (46–59)	42.7 (26–50)	<0.001
Age at onset (y)	31.2 (16–56)	61.4 (57–67)	54.4 (39–69)	NA	NA	NA	15.7 (0–34)	6.5 (0–14)	9.3 (0–30)	<0.001
Disease duration (y)	4.6 (0–22)	1.9 (0–5)	3.0 (1–5)	NA	NA	NA	19.3 (5–47)	46.0 (40–50)	33.5 (15–50)	<0.001
Verbal memory	96.7 (71–108)	83.6 (70–108)	88.8 (78–92)	NA	NA	NA	86.1 (63–100)	90.5 (80–99)	84.5 (77–91)	0.065
Figural memory	88.5 (65–108)	77.5 (61–99)	91.9 (81–107)	NA	NA	NA	84.1 (61–102)	84.3 (75–87)	80.8 (66–87)	0.595
Seizure-free (%)	4 (21)	3 (75)	2 (40)	NA	NA	NA	1 (5)	0 (0)	1 (20)	NA

comorbidities and, most relevant, their response to immunotherapy (Quek et al., 2012). As the presence of pathologic neuronal autoantibodies yet undiscovered may not be excluded by negative antibody testing, diagnostic weight is added on clinical examinations and magnetic resonance imaging (MRI) (Dalmau and Vincent, 2017). Recent research indicates that MRI features of LE depend on the type of autoantibody harbored by the patient. Mesiotemporal structures have been shown to be initially- and predominantly affected by LE; in particular amygdala and hippocampal swelling has been described (Ernst et al., 2019; Heine et al., 2015; Wagner et al., 2015; Fredriksen et al., 2018). Besides, there is growing evidence for serospecific structural alterations also in white matter regions caused by the disease. While a recent study investigating white matter features of LE by means of diffusion tensor imaging (DTI) found widespread alterations of diffusivity parameters in patients with GAD-autoantibody associated LE (GAD-LE), no white matter alterations in patients with VGKC-autoantibody associated LE have been observed (Wagner et al., 2016). However, the accuracy of conventional DTI-methods for reflecting the result of pathophysiological processes in white matter remains questionable. Conventional DTI relies on measures averaged across the volume of one voxel, despite the fact that roughly 90% of white matter voxels contain multiple fiber orientations (Jeurissen et al., 2013). To address this issue in the present study, we chose to apply fixel-based analysis, where metrics are derived from the specific estimated fiber orientation distribution for each white matter voxel (Raffelt et al., 2017). Here, two metrics are combined for each distinct fiber population within a voxel: Fiber cross-section (FC) provides information on a macroscale, while fiber density (FD) assesses microstructural properties. By combining information on both scales, we hypothesized fixel-based analysis to draw a more detailed picture of white matter alterations to enhance future diagnostics. Studies applying fixel-based analysis to patients with hippocampal sclerosis (HS) found tract-specific atrophy on both hemispheres (Vaughan et al., 2017). In this study, we aimed to compare GAD-LE, LGI1-associated LE (LGI1-LE), CASPR2-associated LE (CASPR2-LE), chronic temporal lobe epilepsy patients with HS and healthy controls to investigate the disturbed structure–function relationship, hoping to unmask structural underpinnings of clinical and neuropsychological alterations in LE patients.

2. Materials and methods

2.1. Study groups

This study comprised three experimental and two control groups: GAD-LE, LGI1-LE and CASPR2-LE formed three study groups. Patients with hippocampal sclerosis (HS) and healthy subjects constituted two control groups. First, we prospectively ascertained 19 patients with GAD-LE (mean age = 35.9 years, 11 females), 4 patients with LGI1-LE (mean age = 63.3, 2 females) and 5 patients with CASPR2-LE (mean age = 57.4, 0 females) who presented at the Department of Epileptology at the University Hospital Bonn between April 2008 and November 2016. All patients included in this study were diagnosed with autoimmune limbic encephalitis according to the widely acknowledged diagnostic criteria set forth by Graus et al. (2016). Results of conventional DTI-analysis of a partly overlapping study group were previously published by Wagner et al. (2016). Moreover, autoantibodies against either GAD, LGI1 or CASPR2 were serologically proven in all patients included in this study (see below). Disease onset was defined as the onset of the first LE-associated symptoms. Second, we included 20 matched patients (mean age = 34.1, 11 females) with histologically confirmed HS and no suspicion of LE who presented for presurgical evaluation at our department between May 2008 and October 2013. This additional control group was included since we aimed to specifically detect autoimmune-mediated structural alterations caused by the respective autoantibodies and not those alterations that occur due to persistent temporal lobe epilepsy. HS subjects were individually matched to GAD-, LGI1- and CASPR2-LE with respect to the age at study, gender and the affected hemisphere. Subjects with dual pathologies were excluded from the study. Third, we composed three age- and gender-matched groups of healthy subjects with no history of neurological or psychiatric disorders from a pre-existing in-house database to be contrasted to GAD-LE, LGI1-LE and CASPR2-LE, respectively (GAD-LE healthy controls: mean age = 34.6 years, 11 females; LGI1-LE healthy controls: mean age = 57.0 years, 4 females; CASPR2-LE healthy controls: mean age = 57.2 years, 0 females). For the LGI1-LE and CASPR2-LE healthy control groups, two healthy subjects were matched to each patient to increase statistical power. Clinical data of all patients including memory performance (Verbal memory: VLMT; Helmstaedter et al. (2001), figural memory: DCS-R; Helmstaedter et al. (1991)) were retrieved from our in-house database. See Table 1 for groups characteristics (further details are provided in Supplementary Tables S1–S4). The study was approved by the Internal Review Board of the University Hospital Bonn and all participants provided written informed consent.

2.2. Antibody testing

From 2014 on, screening for onco-neuronal antibodies was performed using semiquantitative immunoblots (EUROLINE PNS 12, Euroimmun, DL 1111–1601-7 G) coated with recombinant antigen or antigen fragments (dilution: serum 1:100, cerebrospinal fluid: 1:1). Moreover, immunocytochemistry was performed using HEK293-cells (Human Embryonic Kidney 293) with expression of antigens on the cell surface (IIFT: Autoimmune-Enzephalitis-Mosaik1, Euroimmun, FA

1120–1005-1; GAD65-IIFT, Euroimmun, FA 1022–1005-50) for NMDAR-, CASPR, LGI1, GABAA-, GABAB-, AMPAR- and GAD65-autoantibodies (dilution: serum 1:10, cerebrospinal fluid: 1:1). Before 2014, detection of GAD antibodies in serum was performed by using an Anti-125 I-GAD-radioimmunoprecipitation assay (normal values ≤ 1 U/ml; Weatherall Institute, Oxford, UK, or Euroimmun, Lübeck, Germany). VGKC-complex antibodies were detected by radioimmunoprecipitation assay (normal values < 100 pM; Weatherall Institute or Euroimmun). Antibodies against LGI1 and CASPR2 were examined by indirect immunofluorescence using formalin fixed HEK293 cells containing membrane bound LGI1 or CASPR2 (normal values $<1:10$; all tests performed by Euroimmun).

2.3. Neuropsychological assessment

Neuropsychological testing was performed within 100 days of the scan. Abilities in figural learning and the overall memory performance were assessed using the revised *Diagnosticum fuer Cerebralschaedigung* (DCR-R; Helmstaedter et al. (1991)). Abilities in verbal learning and the overall memory performance were assessed using the verbal learning and memory test (VLMT; Helmstaedter et al. (2001)). Memory parameters were standardized according to a conormalization sample of 488 healthy volunteers (mean = 100, standard deviation = 10), applying a correction for age.

2.4. MRI examinations

Diffusion Tensor Imaging (DTI) for all subjects was performed at the Life & Brain Center in Bonn using a 3 Tesla MRI-Scanner (Magnetom Trio, Siemens Healthineers, Erlangen, Germany). Diffusion-weighted data were acquired using single shot spin-echo echo-planar imaging. Due to a scanner update in early 2014, two different acquisition protocols were used. Parameters before the update were TR = 12 s, TE = 100 ms using an eight channel headcoil, parameters after the update were TR = 9 s, TE = 87 ms using a 32 channel headcoil. Both protocols acquired 72 axial slices, matrix 128 × 128, voxel size 1.72 mm × 1.72 mm × 1.7 mm and in both protocols, diffusion weighting was isotropically distributed along 60 directions at $b = 1000\ s \cdot mm^{-2}$. Six images with $b = 0$ were acquired initially and following each series of ten diffusion-weighted images. Healthy control groups were matched with regard to sequences before and after the scanner update.

2.5. Reorientation of images

Cortical reconstruction and volumetric segmentation of T1-weighted images was performed using FreeSurfer (version 6.0; Fischl et al. (2002); http://surfer.nmr.mgh.harvard.edu). As it remains unclear whether LE is a predominantly unihemispheric process (Navarro et al., 2016), we defined either the right, the left or both hemispheres as *affected* hemispheres using a two-step classification scheme according to Ernst et al. (2019). Interictal EEG data acquired during the same hospital stay as the MRI examination were used as primary criterion: The hemispheres presenting pathological interictal EEG potentials were classified as the *affected* hemisphere. If EEG data were not available, we used the right/left amygdala volumetric ratio, calculated as $2(V_R - V_L)/(V_R + V_L)$, as a secondary criterion: If the amygdala volumetric ratio was in the upper quartile as compared to controls, the right hemisphere was defined as *affected* hemisphere. If the amygdala volumetric ratio was in the lower quartile as compared to controls, the left hemisphere was defined as *affected* hemisphere. In between, we regarded both hemispheres as *affected*. For whole-brain fixel-based analysis and subsequent group-wise comparisons, we flipped all LE and HS patients with affected right hemispheres along the left–right axis. For ROI-wise correlation analysis with neuropsychological tests, we used the native (unflipped) image orientation.

2.6. Fixel-based preprocessing

Fixel-based analysis was performed using the MRtrix3 toolbox (The Florey Institute, Melbourne, Australia; http://mrtrix.readthedocs.io). The principle behind this approach is to use constrained spherical deconvolution and probabilistic tractography to compute metrics on anatomically plausible fiber populations. Preprocessing of diffusion-weighted images included denoising (Veraart et al., 2016), motion and eddy current distortion correction (Andersson et al., 2003; Andersson and Sotiropoulos, 2016) using the FMRIB software library (FSL, Version 5.0; Jenkinson et al. (2012); http://www.fmrib.ox.ac.uk/fsl) and N4 bias field correction (Tustison et al., 2011). Next, we performed group intensity normalization to the median white matter b = 0 signal and upsampled images to $(1.3\ mm)^3$ voxel size in order to improve downstream spatial normalization statistics. We computed a group average single-shell white matter response function (Tournier et al., 2013), performed constrained spherical deconvolution (Jeurissen et al., 2014) in order to estimate the fiber orientation distribution function (FOD) for all subjects and generated a study-specific group FOD template from a representative subgroup comprising 45 images. FOD template and subject FOD images were segmented to discrete fixels (Smith et al., 2013). Subject FOD and all subsequent images were then registered to the group template. Subsequently, we calculated values for FD (Raffelt et al., 2012), and FC (Raffelt et al., 2017) for all subject fixel images. Furthermore, we computed fiber density and cross-section as FDC = FD · FC and ln(FC) images. ln(FC) images were computed to ensure data were normally distributed and centered around zero for downstream statistical analysis. We performed whole-brain probabilistic tractography on the FOD template selecting $20 \cdot 10^6$ streamlines with a length between 10 and 250 mm and a maximum angle of 22.5°. To correct for tractography biases, we performed spherical deconvolution informed filtering (Smith et al., 2013) and reduced the number of streamlines to $2 \cdot 10^6$. See Fig. 1 for an overview on the processing pipeline. We tested for differences in FD and FC fixel values between both MRI acquisition setups used and did not find any differences within the healthy control group.

2.7. Statistical analysis

Analysis was conducted following a two-tier strategy: First, fixel-wise analysis was conducted and, second, mean fixel values of resulting clusters were used for ROI-wise group comparisons or correlation analysis with neuropsychological assessment metrics. Cross-sectional statistical analysis of fixel-based metrics was performed using connectivity-based fixel enhancement (Raffelt et al., 2015, parameters: $C = 0.75$, $E = 3.5$, $H = 4$) and fixel-wise non-parametric permutation testing (5000 permutations) with the MRtrix3 toolbox. By smoothing and enhancing fixels along the template streamlines, this method puts additional weight on local fixel-fixel connectivity and determines significant fixels that are structurally connected. Second, fixels from resulting clusters were extracted, averaged, and subjected to ROI-wise comparisons and correlation analysis: For comparison of means of independent numerical data across more than two groups, we used one-way analysis of variance and post-hoc Tukey-Kramer test for pair-wise comparisons including a correction for multiple comparisons. Correlation analysis was carried out using Pearson correlation and Steiger's *Z*-test. The Holm-Bonferroni procedure was applied to adjust *p*-values for multiple testing (Holm, 1979). ROI-wise statistical analyses were performed using Stata 14 (Stata Statistical Software: Release 14, StataCorp LP, College Station, TX, USA). In this study, we regard a probability value $p < 0.05$ as statistically significant.

3. Results

3.1. Clinical group differences

All study groups were compared using one-way analysis of variance

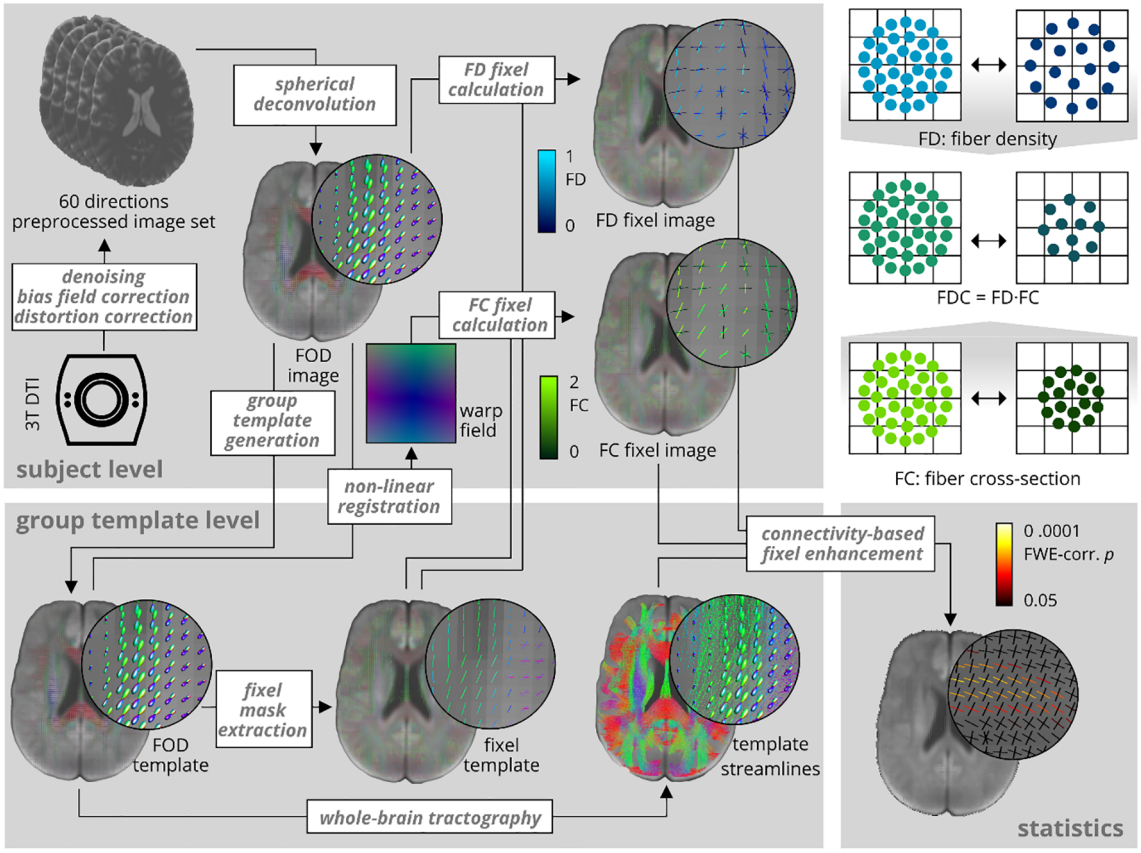

Fig. 1. Overview over the processing pipeline. Fixel-based analysis was performed using the MRtrix3 toolbox. It was conducted as proposed by Raffelt et al. (2017). FC: fiber cross-section, FD: fiber density, FOD: Fiber orientation distribution.

with Tukey-Kramer post-hoc pairwise testing. Between LE groups, we found a significantly lower age at study and age at disease onset in GAD-LE as compared to LGI1-LE (age at study: Tukey-Kramer $p < 0.001$, age at disease onset: Tukey-Kramer $p < 0.001$) and CASPR2-LE (age at study: Tukey-Kramer $p < 0.001$, age at disease onset: Tukey-Kramer $p < 0.001$). Disease duration did not differ significantly neither between GAD-LE and LGI-LE (Tukey-Kramer $p = 0.994$) nor between GAD-LE and CASPR2-LE (Tukey-Kramer $p = 0.999$). Between LE groups and the matched HS groups, in all LE groups the age at disease onset was significantly higher and disease duration was significantly shorter as compared to the matched HS group (all Tukey-Kramer $p < 0.001$). LE groups and HS control groups did not differ significantly in verbal memory performance ($F(5,50) = 2.23$, $p = 0.065$) or figural memory performance ($F(5,50) = 0.74$, $p = 0.595$).

3.2. Fixel values group differences between GAD-LE and control groups

Fixel-wise group comparisons revealed three clusters with significantly lower FDC in GAD-LE versus controls: First and second, we found a significant reduction of FDC in fibers associated to the superior longitudinal fascicle (SLF) on both the *affected* (1) and *unaffected* (2) hemispheres with an average reduction of −5.4% in the *affected* ($t_{max} = 4.57$, $p_{min} = 0.036$, FWE-corrected) and −5.0% in the *unaffected* hemisphere ($t_{max} = 5.25$, $p_{min} = 0.002$, FWE-corrected). Third, we found a significant reduction of FDC in crossing fibers (3) located in the isthmus of the corpus callosum ($t_{max} = 4.88$, $p_{min} = 0.012$, FWE-corrected; see Fig. 2A). FDC reduction was driven by a reduction of both FD and FC (see Supplementary Table S5). In a second step, we projected the (more extensive) SLF-cluster in the *unaffected* hemisphere cluster to the contralateral/*affected* hemisphere, extracted and averaged fixels from both clusters and computed whole-brain-corrected FDC fixel values within the SLF on both hemispheres. Consecutive ROI-wise analysis of covariance adjusting for age and post-hoc pairwise testing confirmed significantly lower bihemispheric FDC values in GAD-LE patients ($F(9,152) = 6.57$, $\eta^2 = 0.28$, $p < 0.001$; see Fig. 2B and Supplementary Table S6) as compared to healthy controls (Tukey-Kramer, *affected* hemisphere: $p < 0.001$, *unaffected* hemisphere: $p = 0.029$). ROI-wise analysis of control patients with HS showed unilaterally lower FDC values only in the *affected* hemisphere as compared to healthy controls (Tukey-Kramer, $p < 0.001$). ROI-wise analysis of CASPR2-LE patients also revealed unilaterally lower FDC values only in the *affected* hemisphere as compared to healthy controls (Tukey-Kramer, $p = 0.003$), the *unaffected* hemisphere in LGI1-LE (Tukey-Kramer, $p = 0.015$) and the *unaffected* hemisphere in HS (Tukey-Kramer, $p = 0.042$). In a second analysis of covariance adjusting all LE and HS groups for age and seizure freedom ($F(9,86) = 2.71$, $\eta^2 = 0.22$, $p = 0.008$; see Supplementary Table S7), lower FDC values in the *affected* hemisphere in CASPR2-LE than in the *unaffected* hemisphere in LGI1-LE remained significant (Tukey-Kramer, $p = 0.013$), whereas the *affected* hemisphere in CASPR2-LE did no longer show significantly lower FDC values than the *unaffected* hemisphere in HS (Tukey-Kramer, $p = 0.211$). After adjusting for seizure freedom, we found significantly lower FDC values in the *affected* hemisphere in HS patients than in the *unaffected* hemisphere in LGI1-LE (Tukey-Kramer, $p = 0.035$).

3.3. Fixel values group differences between LGI1-LE and control groups

Fixel-wise group comparison did not reveal any cluster with significantly different FD, ln(FC) or FDC neither between LGI1-LE and healthy controls ($p_{min} > 0.05$, FWE-corrected) nor between LGI1-LE and HS ($p_{min} > 0.05$, FWE-corrected).

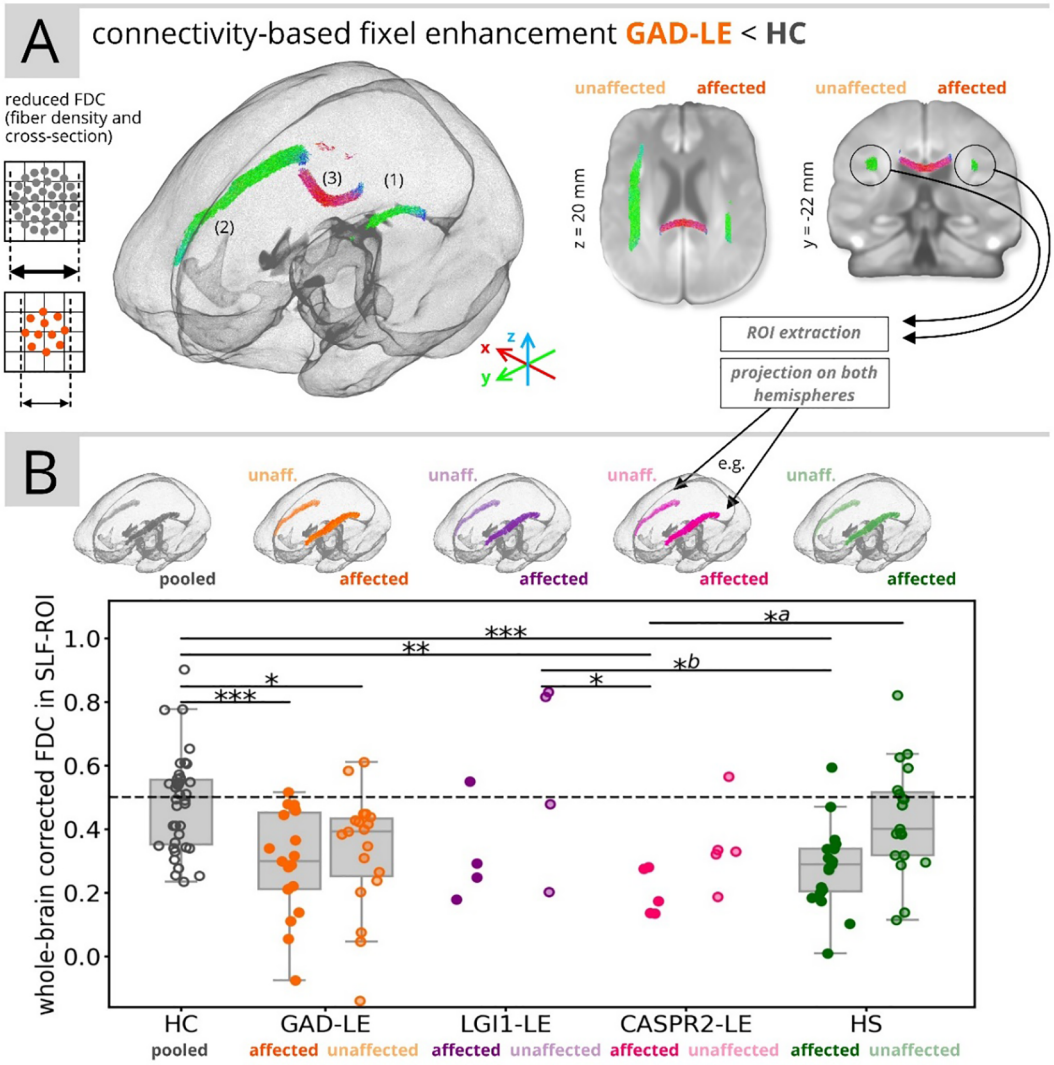

Fig. 2. Summary of fixel-based analysis results. (A) Display of streamlines associated to fixels with significant ($p < 0.05$, FWE-corrected) reduction of FDC in GAD-LE versus controls. (B) Whole-brain corrected mean FDC values in the extracted superior-longitudinal-fascicle-ROI for all groups are shown. [a]Results did not remain significant after adjusting for seizure freedom. [b]Results was only significant after adjusting for seizure freedom. HC: healthy controls; HS: control patients with hippocampal sclerosis; unaff.: unaffeceted; *: $p < 0.05$, **: $p < 0.01$, ***: $p < 0.001$.

3.4. Fixel values group differences between CASPR2-LE and control groups

Fixel-wise group comparison did not reveal any cluster with significantly different FD, ln(FC) or FDC between CASPR2-LE and healthy controls ($p_{min} > 0.05$, FWE-corrected). While FD did not differ significantly between CASPR2-LE and HS, we found a small cluster of significantly higher ln(FC) and FDC in the cerebellar peduncle on CASPR2-LE versus HS ($t_{max} = 10.16$, $p_{min} = 0.01$, FWE-corrected).

3.5. Correlation between ROI-wise fixel values and neuropsychological test results

Moreover, we performed correlation analysis in an explorative design between fixel values extracted from the SLF-ROI found in cross-sectional analysis and neuropsychological scores within the GAD-LE group (see Fig. 3 and Supplementary Table S8). For this analysis, as memory is known to be lateralized, we used a "native" left/right orientation in addition to the orientation according to the hemisphere affected by the disease. We found a significant correlation ($R = 0.64$, Holm-Bonferroni corrected $p < 0.048$) between the left/right ratio of whole brain corrected FC values in the SLF and the assessed verbal memory score. We did not find any correlation between hippocampal volumes and figural or verbal memory performance (uncorrected $p > 0.05$).

3.6. Regression of ROI-wise fixel values by clinical features

We performed regression analysis in order to link our finding of lower FDC in the SLF-ROI with clinical features. Within the HS group, FDC values in the SLF in the affected hemisphere were predicted by a linear regression model ($F(2,17) = 5.23$, $p = 0.017$, $R^2 = 0.38$) including disease duration and age at onset as covariates (see Fig. 4). While we found a significant effect of the disease duration ($t = -3.22$, $p = 0.004$), the contribution of age at onset was not significant ($t = -1.55$, $p = 0.140$). Within the GAD-LE group, the same model did not significantly predict FDC values in the SLF neither of the affected hemisphere ($F(2,16) = 0.48$, $p = 0.628$) nor pooled across both hemispheres ($F(2,16) = 0.82$, $p = 0.451$).

4. Discussion

Using the novel approach of fixel-based analysis, our study reveals distinct fiber tract alteration patterns in patients with LE that can be related to the associated antibody. GAD-LE showed bilaterally lower

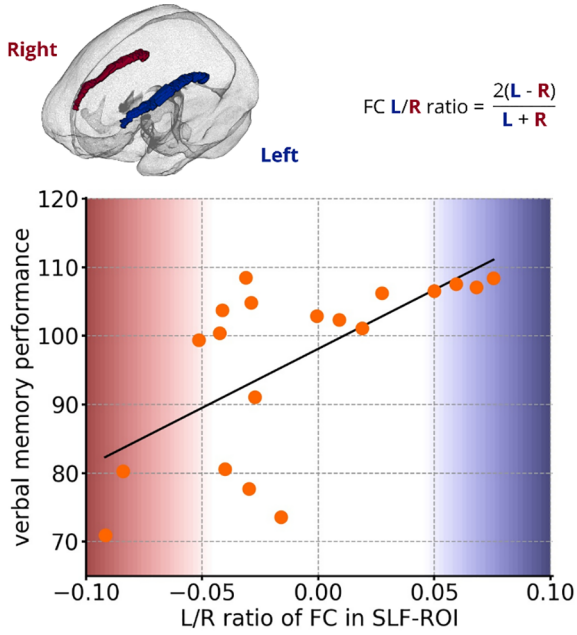

Fig. 3. Results of explorative ROI-wise correlation analysis with neuropsychological performance in the GAD-LE group. Correlation between Left/Right ratio of fiber cross-section values in the extracted SLF-ROI and verbal memory performance (R = 0.64, Holm-Bonferroni corrected p = 0.048; FC: fiber cross-section; SLF: superior longitudinal fascicle; L: left; R: right.

fiber density and cross-section (FDC) in the SLF as compared to healthy controls, while this reduction was present only in the *affected* hemisphere in CASPR2-LE and was not present at all in LGI1-LE. Correlation analysis finally draws a link between the altered SLF and memory performance further suggesting the functional relevance of our findings.

4.1. Clinical group differences

Analyses of clinical features confirm serogroup characteristics previously described in several studies (Malter et al., 2010; Bien et al., 2007; Graus et al., 2016; Dalmau and Graus, 2018): GAD-LE were significantly younger at the onset of the disease than LGI1-LE and CASPR2-LE patients. Also, there were more female patients in the group of GAD-LE (Graus et al., 2016). The disease onset of all LE-groups was much later than in the HS patient control groups, where first symptoms appeared in childhood. As expected, all LE and HS patients equally showed impaired figural and verbal memory performance.

4.2. Fixel-based analysis reflects serostatus

In GAD-LE, widespread reductions of fractional anisotropy have been observed by means of conventional DTI (Wagner et al., 2016). Using fixel-based analysis, this finding could be narrowed down to two fiber tracts affected by significant FDC reduction: Crossing fibers in the isthmus of the corpus callosum and in the SLF in both hemispheres. Reduction of diffusivity parameters in the corpus callosum have been repeatedly observed and discussed (Whelan et al., 2015; Caligiuri et al., 2016). It is subject to an ongoing debate whether they are a consequence of seizures, a part of the underlying pathology, or a contribution of genetics (Vaughan et al., 2017). Structural affection of the *affected* SLF is also known to occur in temporal lobe epilepsy: Reduced FDC of the SLF (Raffelt et al., 2017; Vaughan et al., 2017) and FA reduction (Otte et al., 2012) could be shown by previous studies and is now confirmed by findings in our HS patient control group. The bilateral affection of the SLF found in GAD-LE, however, is novel and may be interpreted as bilateral axonal damage caused by persisting seizures involving a network not limited to the *affected* hemisphere (Ahmadi et al., 2009; Otte et al., 2012; Campos et al., 2015) or as part of the pathologic process in autoimmune encephalitis. In LGI1-LE, a unilateral disease onset is discussed (Navarro et al., 2016; Ernst et al., 2019). Our results, in contrast, failed to reveal any asymmetrical white matter alteration patterns in this group. This might be due to the fact that not all LGI1-LE patients are identified in the early disease stage or due to the very small sample size. Notably, despite small sample sizes, CASPR2-LE showed reduced FDC in the SLF limited to the *affected* hemisphere. Considering the older age at disease onset of LE patients in comparison to HS control patients, it remains open which amount of FDC reduction in the SLF is purely grounded in the autoimmune pathology of LE or simply a consequence of persisting seizures, as it is the case in HS where FDC reduction in the SLF is significantly associated with disease duration. Based on our data, such a link cannot be drawn for LE, especially GAD-LE. Notably, different age at disease onset has been shown to influence the vulnerability of the brain to seizures and the potential for neuroplasticity (Berg et al., 2012; Ben-Ari & Holmes, 2006), which is why the direct comparison between LE subgroups and HS has to be made with caution.

4.3. Functional relevance of structural alterations

We discuss our finding of lower FDC in GAD-LE versus controls located within the SLF in the light of verbal memory performance, a cognitive domain most commonly impaired in temporal lobe epilepsy (Helmstaedter, 2001; Hermann et al., 2006). It is widely recognized that both affected SLF subdivisions, the SLF II and SLFIII, are key components of the dorsal language processing stream and involved in mediating between language functions and working memory (Baddeley, 2000; Bernal and Ardila, 2009; Maldonado et al., 2011; Smits et al., 2014). Our data, showing a positive correlation between the left-greater-than-right asymmetry of FC values within the SLF and verbal memory, is in line with previous studies applying DTI based measures (Vernooij et al., 2007; Catani et al., 2007; Thiebaut de Schotten et al., 2011). This underlines the concept that integrity of superordinated organizational properties of the language processing system rather than isolated damage to one component predicts verbal memory performance (Catani et al., 2007).

4.4. Limitations and outlook

There are three major limitations to the current study. The first limitation lies in the study design: Transversal study designs like the current one are challenged by therapeutic interventions. GAD-LE has been described to be less responsive to immunotherapy as compared to LGI1-LE and CASPR2-LE (Graus et al., 2016). It is, therefore, difficult to discriminate whether differences observed between groups reflect the response to differing treatments or the natural course of the disease. Second, small sample sizes and heterogeneity especially of the LGI1-LE and CASPR2-LE groups limit the ability of the present study to reveal distinct serospecific properties. Notably, because of this limitation, this study did not reveal any significant group differences when comparing LE subgroups against each other. Third, the interpretation of fixel-based measures, mostly in analogy to DTI measures, remains speculative. Yet, in order to increase the value of those metrics as meaningful imaging biomarkers offering pathomechanistic insight, a more detailed understanding of the histopathological underpinnings is essential. Therefore, future studies investigating histolopathological correlates of imaging measures are needed.

5. Conclusion

Imaging research in LE has recently been focused on mesiotemporal gray matter structures. However, in DTI studies it became evident that white matter structures also undergo pathological changes. In the current study, fixel-based analysis has proven to be a useful tool for the

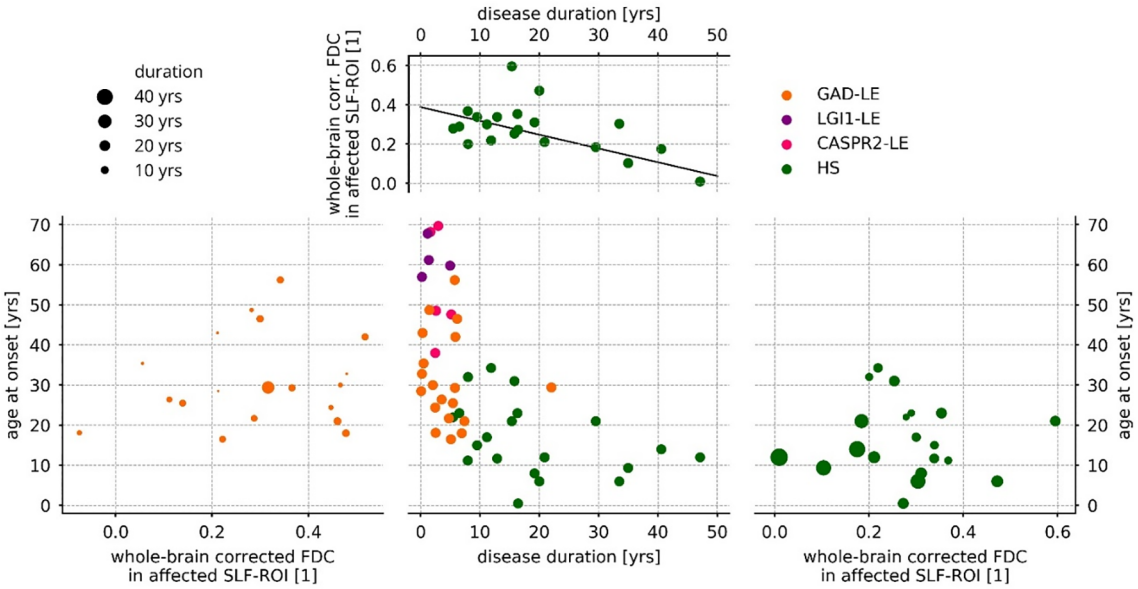

Fig. 4. Results of regression analysis of FDC in the affected superior longitudinal fascicle. Within the hippocampal sclerosis group (right and top), FDC values were predicted ($F(2,17) = 5.23, p = 0.017, R^2 = 0.38$) by disease duration ($t = -3.22, p = 0.004$) and age at onset($t = -1.55, p = 0.140$) , while only the contribution of disease duration was significant (top). Within the GAD-LE group, the same model failed ($F(2,16) = 0.48, p = 0.628$) to predict FDC values in the affected superior longitudinal fascicle (left). FDC: fiber density and cross-section; SLF: superior longitudinal fascicle; yrs: years.

detection of distinct microstructural white matter alterations and could show their functional relevance. It is our hope that the current study, as well as future studies, will help in unveiling the pathomechanism of LE, thereby, strengthening the role of MRI in the diagnosis of LE patients.

Declaration of competing interest

C.E.E. received fees as speaker or consultant from UCB Pharma, Desitin, BIAL and Eisai. R.S. has received fees as speaker or consultant from Bial, Cyberonics, Desitin, Eisai, LivaNova, Novartis, and UCB Pharma.

Acknowledgements

T.B. and L.E. received support from the “BonnNi Promotionskolleg Neuroimmunology” of the University of Bonn and the “Else Kröner-Fresenius-Stiftung” (Grants Nr. 2018-S2-01 and 2016-S2-05). T.R. was supported by the BONFOR research commission of the medical faculty of the University of Bonn. This work was supported by the “Verein zur Förderung der Epilepsieforschung”.

Appendix A. Supplementary data

Supplementary data to this article can be found online at https://doi.org/10.1016/j.nicl.2020.102289.

References

Ahmadi, M.E., Hagler, D.J., McDonald, C.R., Tecoma, E.S., Iragui, V.J., Dale, A.M., Halgren, E., 2009. Side matters: Diffusion tensor imaging tractography in left and right temporal lobe epilepsy. Am. J. Neuroradiol. 30, 1740–1747. https://doi.org/10.3174/ajnr.A1650.

Andersson, J.L., Sotiropoulos, S.N., 2016. An integrated approach to correction for off-resonance effects and subject movement in diffusion MR imaging. Neuroimage 125, 1063–1078. https://doi.org/10.1016/j.neuroimage.2015.10.019.

Andersson, J.L.R., Skare, S., Ashburner, J., 2003. How to correct susceptibility distortions in spin-echo echo-planar images: Application to diffusion tensor imaging. Neuroimage 20, 870–888. https://doi.org/10.1016/S1053-8119(03)00336–7.

Baddeley, A., 2000. The episodic buffer: A new component of working memory? Trends Cogn Sci. 4 417 (423). https://doi.org/10.1016/S1364-6613(00)01538–2.

Ben-Ari, Y., Holmes, G.L., 2006. Effects of seizures on developmental processes in the immature brain. Lancet Neurol. 5 (12), 1055–1063. https://doi.org/10.1016/s1474-4422(06)70626-3.

Berg, A.T., Zelko, F.A., Levy, S.R., Testa, F.M., 2012. Age at onset of epilepsy, pharmacoresistance, and cognitive outcomes. A prospective cohort study. Neurology 79 (13), 1384–1391. https://doi.org/10.1212/WNL.0b013e31826c1b55.

Bernal, B., Ardila, A., 2009. The role of the arcuate fasciculus in conduction aphasia. Brain 132, 2309–2316. https://doi.org/10.1093/brain/awp206.

Bien, C.G., Elger, C.E., 2007. Limbic encephalitis: A cause of temporal lobe epilepsy with onset in adult life. Epilepsy Behav. 10, 529–538. https://doi.org/10.1016/j.yebeh.2007.03.011.

Bien, C.G., Urbach, H., Schramm, J., Soeder, B.M., Becker, A.J., Voltz, R., Vincent, A., Elger, C.E., 2007. Limbic encephalitis as a precipitating event in adult-onset temporal lobe epilepsy. Neurology 69 (1236), 1244. https://doi.org/10.1212/01.wnl.0000276946.08412.ef.

Binks, S.N.M., Klein, C.J., Waters, P., Pittock, S.J., Irani, S.R., 2017. LGI1, CASPR2 and related antibodies: a molecular evolution of the phenotypes. J. Neurol. Neurosurg. Psychiatry 89, 526–534. https://doi.org/10.1136/jnnp-2017-315720.

Caligiuri, M.E., Labate, A., Cherubini, A., Mumoli, L., Ferlazzo, E., Aguglia, U., Quattrone, A., Gambardella, A., 2016. Integrity of the corpus callosum in patients with benign temporal lobe epilepsy. Epilepsia 57, 590–596. https://doi.org/10.1111/epi.13339.

Campos, B.M., Coan, A.C., Beltramini, G.C., Liu, M., Yassuda, C.L., Ghizoni, E., Beaulieu, C., Gross, D.W., Cendes, F., 2015. White matter abnormalities associate with type and localization of focal epileptogenic lesions. Epilepsia 56, 125–132. https://doi.org/10.1111/epi.12871.

Catani, M., Allin, M.P.G., Husain, M., Pugliese, L., Mesulam, M.M., Murray, R.M., Jones, D.K., 2007. Symmetries in human brain language pathways correlate with verbal recall. Proc. Natl. Acad. Sci. 104, 17163–17168. https://doi.org/10.1073/pnas.0702116104.

Dalmau, J., Graus, F., 2018. Antibody-mediated encephalitis. N. Engl. J. Med. 378, 840–851. https://doi.org/10.1056/NEJMra1708712.

Dalmau, J., Vincent, A., 2017. Do we need to measure specific antibodies in patients with limbic encephalitis? Neurology 88, 508–509. https://doi.org/10.1212/WNL.0000000000003592.

Dubey, D., Pittock, S.J., Kelly, C.R., McKeon, A., Lopez-Chiriboga, A.S., Lennon, V.A., Gadoth, A., Smith, C.Y., Bryant, S.C., Klein, C.J., Aksamit, A.J., Toledano, M., Boeve, B.F., Tillema, J.M., Flanagan, E.P., 2018. Autoimmune encephalitis epidemiology and a comparison to infectious encephalitis. Ann. Neurol. 83, 166–177. https://doi.org/10.1002/ana.25131.

Ernst, L., David, B., Gaubatz, J., Elger, C.E., Rüber, T., 2019. Volumetry of Mesiotemporal Structures Reflects Serostatus in Patients with Limbic Encephalitis. Am. J. Neuroradiol. doi:10.3174/ajnr.A6289 [in press].

Fischl, B., Salat, D., Busa, E., Albert, M., Dieterich, M., Haselgrove, C., Van der Kouwe, A., Killiany, R., Kennedy, D., Klaveness, S., Montillo, A., Makris, N., Rosen, B., Dale, A., 2002. Whole brain segmentation: Automated labeling of neuroanatomical structures in the human brain. Neuron 33 (3), 341–355. https://doi.org/10.1016/s0896-6273(02)00569-x.

Fredriksen, J.R., Carr, C.M., Koeller, K.K., Verdoorn, J.T., Gadoth, A., Pittock, S.J., Kotsenas, A.L., 2018. MRI findings in glutamic acid decarboxylase associated autoimmune epilepsy. Neuroradiology 60, 239–245. https://doi.org/10.1007/s00234-018-1976-6.

Graus, F., Saiz, A., Dalmau, J., 2010. Antibodies and neuronal autoimmune disorders of the CNS. J. Neurol. 257, 509–517. https://doi.org/10.1007/s00415-009-5431-9.

Graus, F., Titulaer, M.J., Balu, R., Benseler, S., Bien, C.G., Cellucci, T., Cortese, I., Dale, R.C., Gelfand, J.M., Geschwind, M., Glaser, C.A., Honnorat, J., Höftberger, R., Iizuka, T., Irani, S.R., Lancaster, E., Leypoldt, F., Prüss, H., Rae-Grant, A., Reindl, M.,

Rosenfeld, M.R., Rostásy, K., Saiz, A., Venkatesan, A., Vincent, A., Wandinger, K.P., Waters, P., Dalmau, J., 2016. A clinical approach to diagnosis of autoimmune encephalitis. Lancet Neurol. 15, 391–404. https://doi.org/10.1016/S1474-4422(15)00401-9.

Heine, J., Prüss, H., Bartsch, T., Ploner, C.J., Paul, F., Finke, C., 2015. Imaging of autoimmune encephalitis - Relevance for clinical practice and hippocampal function. Neuroscience 309, 68–83. https://doi.org/10.1016/j.neuroscience.2015.05.037.

Helmstaedter, C., 2001. Neuropsychological complaints, deficits, and difficulties in everyday, in: Fäfflin, M., Fraser, R., Thorbecke, R., Specht, U., Wolf, P. (Eds.), Compr. Care People With Epilepsy, pp. 293–306.

Helmstaedter, C., Lendt, M., Lux, S., 2001. VLMT Verbaler Lern- und Merkfaehigkeitstest. Beltz Test GmbH, Goettingen.

Helmstaedter, C., Pohl, C., Hufnagel, A., Elger, C., 1991. visual learning deficits in non-resected patients with right temporal lobe epilepsy. Cortex 27, 547–555. https://doi.org/10.1016/S0010-9452(13)80004-4.

Hermann, B.P., Seidenberg, M., Dow, C., Jones, J., Rutecki, P., Bhattacharya, A., Bell, B., 2006. Cognitive prognosis in chronic temporal lobe epilepsy. Ann. Neurol. 60, 80–87. https://doi.org/10.1002/ana.20872.

Holm, S., 1979. A simple sequentially rejective multiple test procedure. Scandinavian J. Stat. 6 (2), 65–70.

Irani, S.R., Alexander, S., Waters, P., Kleopa, K.A., Pettingill, P., Zuliani, L., Peles, E., Buckley, C., Lang, B., Vincent, A., 2010. Antibodies to Kv1 potassium channel-complex proteins leucine-rich, glioma inactivated 1 protein and contactin-associated protein-2 in limbic encephalitis Morvan's syndrome and acquired neuromyotonia. Brain 133 (9), 2734–2748. https://doi.org/10.1093/brain/awq213.

Jenkinson, M., Beckmann, C.F., Behrens, T.E., Woolrich, M.W., Smith, S.M., 2012. FSL. Neuroimage 62, 782–790. https://doi.org/10.1016/J.NEUROIMAGE.2011.09.015.

Jeurissen, B., Leemans, A., Tournier, J.D., Jones, D.K., Sijbers, J., 2013. Investigating the prevalence of complex fiber configurations in white matter tissue with diffusion magnetic resonance imaging. Hum. Brain Mapp. 34, 2747–2766. https://doi.org/10.1002/hbm.22099.

Jeurissen, B., Tournier, J.D., Dhollander, T., Connelly, A., Sijbers, J., 2014. Multi-tissue constrained spherical deconvolution for improved analysis of multi-shell diffusion MRI data. Neuroimage 103, 411–426. https://doi.org/10.1016/j.neuroimage.2014.07.061.

Lai, M., Huijbers, M.G., Lancaster, E., Graus, F., Bataller, L., Balice-Gordon, R., Cowell, J.K., Dalmau, J., 2010. Investigation of LGI1 as the antigen in limbic encephalitis previously attributed to potassium channels: A case series. Lancet. Neurol. 9 (8), 776–785. https://doi.org/10.1016/S1474-4422(10)70137-X.

Maldonado, I.L., Moritz-Gasser, S., Duffau, H., 2011. Does the left superior longitudinal fascicle subserve language semantics? A brain electrostimulation study. Brain Struct. Funct. 216, 263–274. https://doi.org/10.1007/s00429-011-0309-x.

Malter, M.P., Helmstaedter, C., Urbach, H., Vincent, A., Bien, C.G., 2010. Antibodies to glutamic acid decarboxylase define a form of limbic encephalitis. Ann. Neurol. 67, 470–478. https://doi.org/10.1002/ana.21917.

Navarro, V., Kas, A., Apartis, E., Chami, L., Rogemond, V., Levy, P., Psimaras, D., Habert, M.O., Baulac, M., Delattre, J.Y., Honnorat, J., Collaborators,, 2016. Motor cortex and hippocampus are the two main cortical targets in LGI1-antibody encephalitis. Brain 139, 1079–1093.

Otte, W.M., Van Eijsden, P., Sander, J.W., Duncan, J.S., Dijkhuizen, R.M., Braun, K.P., 2012. A meta-analysis of white matter changes in temporal lobe epilepsy as studied with diffusion tensor imaging. Epilepsia 53, 659–667. https://doi.org/10.1111/j.1528-1167.2012.03426.x.

Quek, A.M.L., Britton, J.W., McKeon, A., So, E., Lennon, V.A., Shin, C., Klein, C., Watson, R.E., Kotsenas, A.L., Lagerlund, T.D., Cascino, G.D., Worrell, G.A., Wirrell, E.C., Nickels, K.C., Aksamit, A.J., Noe, K.H., Pittock, S.J., 2012. Autoimmune epilepsy: clinical characteristics and response to immunotherapy. Arch. Neurol. 69, 582–593. https://doi.org/10.1001/archneurol.2011.2985.

Raffelt, D.A., Smith, R.E., Ridgway, G.R., Tournier, J.D., Vaughan, D.N., Rose, S., Henderson, R., Connelly, A., 2015. Connectivity-based fixel enhancement: Whole-brain statistical analysis of diffusion MRI measures in the presence of crossingfibres. Neuroimage 117, 40–55. https://doi.org/10.1016/j.neuroimage.2015.05.039.

Raffelt, D.A., Tournier, J.D., Rose, S., Ridgway, G.R., Henderson, R., Crozier, S., Salvado, O., Connelly, A., 2012. Apparent Fibre Density: A novel measure for the analysis of diffusion-weighted magnetic resonance images. Neuroimage 59, 3976–3994. https://doi.org/10.1016/j.neuroimage.2011.10.045.

Raffelt, D.A., Tournier, J.D., Smith, R.E., Vaughan, D.N., Jackson, G., Ridgway, G.R., Connelly, A., 2017. Investigating white matter fibre density and morphology using fixel-based analysis. Neuroimage 144, 58–73. https://doi.org/10.1016/j.neuroimage.2016.09.029.

Smith, R.E., Tournier, J.D., Calamante, F., Connelly, A., 2013. SIFT: Spherical-deconvolution informed filtering of tractograms. Neuroimage 67, 298–312. https://doi.org/10.1016/j.neuroimage.2012.11.049.

Smits, M., Jiskoot, L.C., Papma, J.M., 2014. White Matter Tracts of Speech and Language. Semin. Ultrasound, CT MRI 35, 504–516. https://doi.org/10.1053/J.SULT.2014.06.008.

van Sonderen, A., Petit-Pedrol, M., Dalmau, J., Titulaer, M.J., 2017. The value of LGI1, Caspr2 and voltage-gated potassium channel antibodies in encephalitis. Nat. Rev. Neurol. 13, 290.

Thiebaut de Schotten, M., Ffytche, D.H., Bizzi, A., Dell'Acqua, F., Allin, M., Walshe, M., Murray, R., Williams, S.C., Murphy, D.G., Catani, M., 2011. Atlasing location, asymmetry and inter-subject variability of white matter tracts in the human brain with MR diffusion tractography. Neuroimage 54, 49–59. https://doi.org/10.1016/J.NEUROIMAGE.2010.07.055.

Tournier, J.D., Calamante, F., Connelly, A., 2013. Determination of the appropriate b value and number of gradient directions for high-angular-resolution diffusion-weighted imaging. NMR Biomed. 26, 1775–1786. https://doi.org/10.1002/nbm.3017.

Tustison, N.J., Cook, P.A., Gee, J.C., 2011. N4ITK: Improved N3 Bias Correction. IEEE Trans Med Imaging 29, 1310–1320. https://doi.org/10.1109/TMI.2010.2046908.N4ITK.

Vaughan, D.N., Raffelt, D., Curwood, E., Tsai, M.H., Tournier, J.D., Connelly, A., Jackson, G.D., 2017. Tract-specific atrophy in focal epilepsy: Disease, genetics, or seizures? Ann. Neurol. 81, 240–250. https://doi.org/10.1002/ana.24848.

Veraart, J., Fieremans, E., Novikov, D.S., 2016. Diffusion MRI noise mapping using random matrix theory. Magn. Reson. Med. 76, 1582–1593. https://doi.org/10.1002/mrm.26059.

Vernooij, M.W., Smits, M., Wielopolski, P.A., Houston, G.C., Krestin, G.P., van der Lugt, A., 2007. Fiber density asymmetry of the arcuate fasciculus in relation to functional hemispheric language lateralization in both right- and left-handed healthy subjects: A combined fMRI and DTI study. Neuroimage 35, 1064–1076. https://doi.org/10.1016/j.neuroimage.2006.12.041.

Wagner, J., Schoene-Bake, J.C., Witt, J.A., Helmstaedter, C., Malter, M.P., Stoecker, W., Probst, C., Weber, B., Elger, C.E., 2016. Distinct white matter integrity in glutamic acid decarboxylase and voltage-gated potassium channel-complexantibody-associated limbic encephalitis. Epilepsia 57, 475–483. https://doi.org/10.1111/epi.13297.

Wagner, J., Weber, B., Elger, C.E., 2015. Early and chronic gray matter volume changes in limbic encephalitis revealed by voxel-based morphometry. Epilepsia 56, 754–761. https://doi.org/10.1111/epi.12968.

Whelan, C.D., Alhusaini, S., O'Hanlon, E., Cheung, M., Iyer, P.M., Meaney, J.F., Fagan, A.J., Boyle, G., Delanty, N., Doherty, C.P., Cavalleri, G.L., 2015. White matter alterations in patients with MRI-negative temporal lobe epilepsy and their asymptomatic siblings. Epilepsia 56, 1551–1561. https://doi.org/10.1111/epi.13103.